Localization in quantum percolation: Transfer-matrix calculations in three dimensions

C. M. Soukoulis,* E. N. Economou,† and Gary S. Grest
Corporate Research Science Laboratory, Exxon Research and Engineering Company, Annandale, New Jersey 08801
(Received 17 June 1987)

The quantum site percolation problem, which is defined by a disordered tight-binding Hamiltonian with a binary probability distribution, is studied using finite-size scaling methods. For the simple cubic lattice, the dependence of the mobility edge on the strength of the site energy is obtained. Exactly at the center of each subband the states appear to be always localized. The lowest value of the quantum site percolation threshold is $p_q = 0.44 \pm 0.01$ and occurs for an energy near the center of the subband. These numerical results are found to be in satisfactory agreement with the predictions of the potential-well analogy, based on a cluster coherent-potential approximation. The integrated density of states is also calculated numerically. A spike in the density of states exactly at the center of the subband and a gap around it are observed, in agreement with earlier work by Kirkpatrick and Eggarter.

I. INTRODUCTION

Considerable interest in recent years has focused on quantum percolation problems.[1-8] Quantum percolation is usually formulated in terms of a tight-binding one-electron Hamiltonian on a regular simple cubic lattice

$$H = \sum_n |n\rangle \varepsilon_n \langle n| + \sum_{\substack{n,m \\ (n \neq m)}} |n\rangle V_{nm} \langle m| , \quad (1)$$

where the transfer energy V_{nm} vanishes unless n and m are nearest neighbors on the lattice and is constant otherwise. We can describe the quantum analogue of the site percolation by constant transfer energy $V_{nm} = 1$ random-site energies obeying the probability distribution

$$p(\varepsilon_n) = p\delta(\varepsilon_n - \varepsilon_A) + (1-p)\delta(\varepsilon_n - \varepsilon_B), \quad \varepsilon_B = -\varepsilon_A . \quad (2)$$

In the classical percolation problem, sites on a lattice are randomly occupied with probability p, and two occupied sites are connected if they are nearest neighbors. It is well-known that there exists a critical value p_c, below which all clusters of connected sites are finite. On the other hand, for $p > p_c$ the probability is unity that there exists an infinite cluster. In quantum percolation the corresponding quantity of interest is the quantum percolation threshold p_q, below which all eigenstates of the Hamiltonian are localized. It is clear that $p_q \geq p_c$, since the existence of an infinite cluster is a necessary condition for the existence of an extended state. There have been many estimates of the quantum percolation threshold p_q for the simple cubic lattice. Early numerical works suggested that p_q was in fact very close to p_c ($p_c = 0.3117 \pm 0.0003$ for a simple cubic lattice[9]). Raghavan[5] using the tridiagonalization method found for the simple cubic lattice $p_q = 0.38$. Srivastava and Chaturvedi[6] found that $p_q = 0.47$ by examining numerically the inverse participation ratio. Odagaki and Chang[7] used a real-space renormalization-group approach to obtain $p_q = 0.70$ and Root and Skinner[8] using a macroscopic renormalization-group method found that $p_q = 0.45$. While the different numerical methods clearly show that indeed p_q is greater than p_c, there is not agreement on its numerical value.

The purpose of the present paper is to make a detailed numerical study of the quantum site percolation process on the basis of the finite-size scaling methods[10-12] using the very reliable transfer-matrix technique. For the simple cubic lattice we numerically obtained the dependence of the critical value of ε_A on the concentration p for $E = \varepsilon_A$. We also calculated, for the first time, the entire mobility edge trajectory in the concentration-energy plane for different values of ε_A. This trajectory is in good agreement with the predictions of the potential-well analogy (PWA) based on a cluster coherent potential approximation (CPA). We also calculate within the CPA, the localization length λ, the correlation length ξ, the mean free path l, and the density of states (DOS) as a function of energy for different concentrations p. Finally, we determined numerically the integrated density of states (DOS) which clearly shows that the DOS exhibits a strong dip around the center of the band as well as a spike exactly at the center.

In Sec. II we briefly describe the formalism and the method of calculation. In Sec. III we present and discuss the results of this calculation. In Sec. IV we present the PWA cluster CPA method and its results and in the final section, we summarize the conclusions of this work.

II. METHOD OF CALCULATION

Up to now, the most reliable numerical technique in obtaining quantitative results in the problem of Anderson localization in disordered systems, is the transfer-matrix method.[10-12] In this method, one considers coupled one-dimensional (1D) systems. Each 1D system is described by a tight-binding Hamiltonian of the form as in Eq. (1). In our explicit results for this study, we as-

sume that the probability distribution $p(\varepsilon_n)$ of the random sites is a sum of two δ functions, as described in Eq. (2). [In previous numerical calculations we[12] have systematically studied the behavior of the tight-binding disordered systems when $p(\varepsilon_n)$ is given by either a rectangular or a Gaussian probability distribution.] The corresponding sites of the nearest-neighbor 1D system are coupled together by an interchain matrix element. As the number of coupled chains approaches infinity, we recover either the two-dimensional (2D) system when the chains are placed on a plane of cross section M with two nearest neighbors each, or the three-dimensional (3D) system when they are placed to form a cylinder of square cross section M^2. For the M regularly placed chains of length N, one determines the largest localization length λ_M as $N\to\infty$. Then from a plot of λ_M versus M one can determine the localization properties of the system.[10-12] In particular, by studying λ_M/M versus M one obtains a reasonable estimate of the mobility edge trajectory. At exactly the mobility edge[10-12] $\lambda_M/M=0.6$ while for extended and localized states we have that λ_M/M versus M increases or decreases, respectively. This criterion has been checked by us[12] for disordered tight-binding models in 3D with a rectangular and Gaussian probability distribution for the site energies.

In addition to our numerical results[11-12] using the transfer matrix, we have also used the PWA based on the simple CPA and on a cluster CPA. We have found that, while the simple CPA gives results with appreciable discrepancies from the numerical ones, the cluster CPA agrees reasonably well with them. The CPA calculates the average Green's function G corresponding to H from an effective periodic Hamiltonian resulting from Eq. (1), by replacing ε_n by a common self-energy Σ, which is determined by a self-consistent equation.[13-15] By this procedure, the self-energy, the Green's function, the mean-free-path length, $l(E)$, the conductivity $\sigma_0(E)$, and the constant energy surface $S(E)$ in 3D, are calculated. The details of this procedure can be found in Refs. 13-15. The results of the CPA are used as input to construct an effective potential well. The depth $V_0(E)$ of the effective potential well is proportional to $\sigma_0^{-1}(E)l^{-D}(E)$, where D is the dimensionality and the width $\alpha(E)$ is proportional to $l(E)$. As we mentioned above, by employing the CPA one can find at every energy E the mean free path $l(E)$ and the CPA conductivity $\sigma_0(E)$; then from $l(E)$ and $\sigma_0(E)$ one can construct the effective potential well characterized by $\alpha(E)$ and $V_0(E)$. If this potential well can sustain a bound state with a decay length $\lambda(E)$ then the eigenstates at E are localized with localization length $\lambda(E)$. If no bound state exists at the effective potential well, the eigenstates of E are extended. In 3D, the mobility-edge energy E, which separates extended from localized states is given by the relation

$$S(E_c)l^2(E_c)=8.96\ . \tag{3}$$

It is important to stress that quantities which have been obtained before[12-14] from the approximate scheme outlined above (based on the CPA and the potential-well analogy) are in satisfactory agreement[12-14] with results based on independent numerical methods. However, in the present case of a binary probability distribution, the simple CPA results for the DOS, $l(E)$, and $\sigma_0(E)$ are not accurate because this probability distribution makes the role of cluster effects very pronounced, while at the same time the CPA omits these effects.

III. NUMERICAL RESULTS AND DISCUSSION

In this section we present results based upon the numerical techniques. We work within the framework of Anderson's model. Thus the input of our study are the following. (i) The lattice structure and quantities associated with the lattice structure such as the number of nearest neighbors Z and the Green's function associated with the periodic Hamiltonian $H=\sum_{n,m}V\,|\,n\,\rangle\langle\,m\,|$. Here we consider the simple cubic lattice where $Z=6$. (ii) The probability distributions of the site energies $p(\varepsilon_n)$. We consider here the case of a binary-alloy type where $p(\varepsilon_n)$ is given by Eq. (2). This probability distribution is essentially characterized by two parameters: p, the concentration of A atoms, i.e., the probability that a given site will be ε_A and ε_A or $\delta=|\varepsilon_A-\varepsilon_B|/ZV=2\varepsilon_A/ZV$, which can be considered as determining the degree of disorder. A case of importance is the binary-alloy distribution when $\delta\to\infty$. In this case, the only way an electron being initially at an A (B) site may propagate to infinity is to find a path consisting entirely of A (B) sites and extending to infinity. Percolation theory examines exactly this problem, i.e., the probability $P(p)$ of finding such an exclusive A path. It turns out that this theory predicts a critical concentration p_c such that $P(p)=0$ for $p<p_c$ and $P(p)>0$ for $p>p_c$, where p_c depends on the particular lattice. For a simple cubic lattice[9] $p_c=0.3117\pm0.003$. According to these remarks, the concentration above which all eigenstates in the A subband as $\delta\to\infty$ are extended must be equal to or greater than p_c. We have systematically calculated the λ_M's for several values of δ, p, and energies E for $M=2-9$. Using the criterion[11,12] that $\lambda_M/M=0.6$ exactly at the mobility edge, we have calculated for the first time the dependence of the mobility edge on the disorder and concentration p. In Fig. 1 we plot δ versus p for $E=\varepsilon_A$, i.e., at the center of the A subband. Figure 1 can be used to describe qualitatively the sequence of events associated with the introduction of impurities in a given crystalline material. If the disorder is not strong enough, i.e., $\delta<2$ or $\varepsilon_A<6V$, then the state at the center of the A subband is always extended independent of the concentration p of the A atoms. For higher disorder, $\delta>2$, as the concentration of impurities increases from zero an impurity subband is formed consisting initially entirely of localized eigenstates, since the eigenstate at the center of the subband is localized. The first extended state at $E=\varepsilon_A$ appears at a higher concentration p of the A atoms and depends on the strength of the disorder. It was expected that in the quantum percolation limit, i.e., $\delta\to\infty$, the quantum percolation threshold p_q would approach a value less than unity. However, as

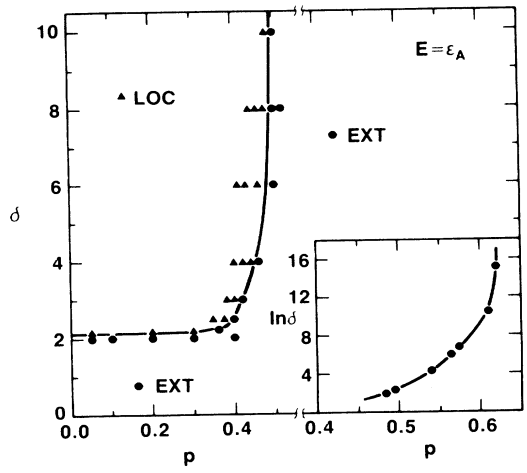

FIG. 1. Phase diagram of the binary-alloy model for $E=\varepsilon_A$. The strength of the disorder $\delta=2\varepsilon_A/6V$ and p is the concentration of the sites with energy ε_A. In the insert of $\ln\delta$vs p is plotted.

one can see from the inset in Fig. 1, p_q continues to increase slowly as δ increases. From the data given in the inset, it is difficult to extract what is the functional dependence of p_q on δ for large δ. It seems that p_q follows either a weakly power-law dependence of the form $p_q=0.7-0.26/\varepsilon_A$ or a logarithmic dependence of the form $p_q=0.64-0.5/\ln(\varepsilon_A)$. However, these fits are only to data up to $\delta=10^7$ and are probably not indicative of the true $\delta\to\infty$ limit. In fact, a very plausible explanation of our data is that, at $E=\varepsilon_A$, p_q is, in fact, equal to 1 for $\delta=\infty$, as was first suggested by Kirkpatrick and Eggarter.[1]

From Fig. 1, we find that if we had used only the data up to $\delta=10$ then we would have erroneously concluded that the threshold at $E=\varepsilon_A$ is at $p_q=0.50$, well above the classical percolation threshold of $p_c=0.3117$, in agreement with some of the previous numerical calculations.[6,8] Most of the previous work, in this problem is based on calculations of the participation ratio[2,4,5] or of the macroscopic renormalization group.[7,8] Both of these methods do not determine the nature of the eigenstate at the center of the A subband. Instead, they average a few eigenstates around the center of the A subband and therefore the values that are obtained for p_q are influenced by the states closer to the center of the subband. For this reason we decided to systematically study the dependence of p_q on the energy of the entire A subband, with the transfer matrix method.[10-12] The results of this study are shown in Fig. 2, where the mobility edge trajectory in the concentration-energy plane is calculated for three different strengths of disorder ε_A. The energy shown in Fig. 2 is measured from the center of the A subband i.e., $E=0$, corresponds to $E=\varepsilon_A$ in Eq. (2). Notice that p_q is very sensitive function of the strength of the disorder ε_A for $E=0$, while there is a much weaker dependence on ε_A for $E\neq 0$. We want to stress again that at the center of the A subband, $E=0$, p_q is most probably equal to 1 in the limit $\varepsilon_A\to\infty$. Within our method of calculation we might not be exactly at the center of the band, since we only do finite systems ($9\times 9\times 6000$) and have an imaginary part in the energy with magnitude of 10^{-4} or 10^{-5}. Notice that in the region $-1<E/2V<1$, p_q is nearly constant with the exception of the sharp peak at $E=0$ and a weak maximum at $|E|/2V\simeq 0.5$ and depends very weakly on ε_A. For $|E|/2V\rangle 1$, we observed no dependence of p_q on ε_A.

Now let us consider some properties of the DOS. For a given p and δ or ε_A the DOS has the following form. For zero disorder, $\delta=\varepsilon_A=0$, there is a single band spanning from $E=-6V$ to $6V$ for the simple cubic lattice. As the disorder increases the DOS remains a single band which is a uniformly stretched version of the unperturbed DOS. For even stronger disorder, $\delta\geq 2$, the single band splits into two bands approximately centered at $-\varepsilon_A$ and ε_A with widths approximately equal to $2ZVp$ and $2ZV(1-p)$. CPA results show this behavior[16,17] as well as the numerical results of Kirkpatrick and Eggarter.[1] Another very interesting feature of the DOS is an obvious spike in the center of the subband and gap regions on both sides of the central spike in which no states are found.[1] Both the gap and the spike became narrower when the concentration is increased for samples of a given size. Finally, for large enough concentrations the dip is no longer apparent.

We have undertaken[18] a systematic study of the integrated DOS for the binary probability distribution as well as for other distributions to check the universality ideas in the tails of DOS in disordered systems. Here we only present how the spike at the center of subband and the gaps around the spike depend on the strength of the disorder ε_A for a given concentration $p=0.30$. This is clearly shown in Fig. 3 where the IDOS versus energy is plotted for different values of ε_A. Notice that for small values of ε_A ($5V$ and $8V$), there is only a very weak signature of a gap around the center of the subband and no

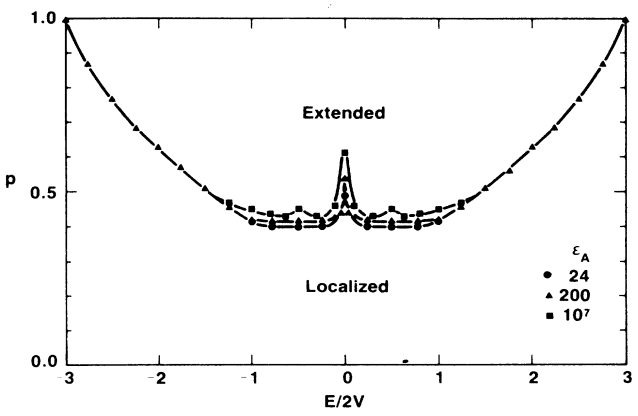

FIG. 2. Mobility-edge trajectory in the concentration-energy plane for the binary-alloy model in a simple cubic system for three values of the disorder strength.

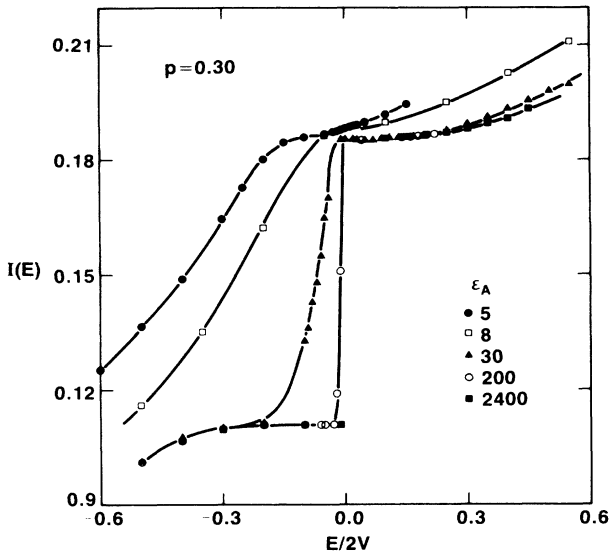

FIG. 3. Integrated density of states vs energy for the binary-alloy system in a simple cubic system at $p=0.30$ for five values of the disorder strength.

spike at $E=0$. By $\varepsilon_A=30V$, a spike has clearly developed, as seen by the large jump in Fig. 3 for the IDOS. The gap around the center of the subband is clearly seen for $\varepsilon_A=200V$ and $2400V$.

IV. PWA RESULTS AND DISCUSSION

The potential well analogy (PWA) leads[13] to Eq. (3) for the determination of the mobility edge. The quantities $l(E)$ and $S(E)$ in Eq. (3) are obtained within the framework of the simple CPA as follows.

The effective site energy $\varepsilon_A-\Sigma$ is determined from the equation

$$\left\langle \frac{\varepsilon_n-\varepsilon_A+\Sigma}{1-(\varepsilon_n-\varepsilon_A+\Sigma)G(E)} \right\rangle=0 , \tag{4}$$

where the average is over the probability distribution of ε_n and G is given by

$$G(E)=G_0(E-\varepsilon_A+\Sigma) , \tag{5}$$

$G(E-\varepsilon_0)$ is the periodic site diagonal Green's function for a band centered at ε_0. Then we have

$$v(E)=v_0(E-\varepsilon_A+\mathrm{Re}\Sigma) , \tag{6}$$

$$S(E)=S_0(E-\varepsilon_A+\mathrm{Re}\Sigma) , \tag{7}$$

$$l(E)=v(E)\tau(E) , \tag{8}$$

$$\tau(E)=\hbar/2\,|\,\mathrm{Im}\Sigma(E)\,| . \tag{9}$$

The quantities $S_0(E-\varepsilon_0)$ and $v_0(E-\varepsilon_0)$ are the area in k space of the surface of constant energy E and the average of the velocity $|\mathbf{v}_k|$ over the same surface for a periodic tight-binding band centered around ε_0. If one assumes that v_0 is the same as the inverse of the average of $|\mathbf{v}_k|^{-1}$ then one obtains

$$S_0=(2\pi)^3\hbar(\rho_0\rho_{02})^{1/2} , \tag{10}$$

$$v_0\simeq\left[\frac{\rho_{02}}{\rho_0}\right]^{1/2} , \tag{11}$$

where

$$\rho_{02}(E-\varepsilon_0)=\int d^3k\,\delta(E-E_k)v_k^2/(2\pi)^3 ,$$

and

$$\rho_0(E-\varepsilon_0)=\int d^3k\,\delta(E-E_k)/(2\pi)^3 .$$

The quantities ρ_{02} and ρ_0 can be expressed in terms of matrix elements of the unperturbed Green's functions.[13]

Explicit results have been obtained both for the simple cubic case and the simple case (not corresponding to a real lattice) for which $E_k=2\sqrt{3}V\cos(|\mathbf{k}|/\sqrt{3})$. The latter case allows explicit analytical results for the unperturbed case:

$$\rho_0(E)=|C(E)|^{1/2}/3\pi a^3V , \tag{12}$$

$$v_0(E)=2\sqrt{3}aV\,|C(E)|^{1/2}/\hbar , \tag{13}$$

$$S_0(E)=16\pi^2\,|C(E)|/\sqrt{3}a^2 , \tag{14}$$

where $C(E)=1-(E/6V)^2$ and a is the "lattice" spacing.

In the limit $\varepsilon_A\to\infty$, Eq. (4) reduces to

$$G\Sigma=1-p , \tag{15}$$

which can be solved explicitly in the particular case of Eqs. (12)–(14) to give

$$\rho(E)=\frac{1}{3\pi Va^3}\left|p-\left[\frac{E-\varepsilon_A}{6V}\right]^2\right|^{1/2} , \tag{16}$$

for

$$|E-\varepsilon_A|\le 6V\sqrt{p} , \tag{17}$$

$$l(E)=\frac{a\sqrt{p}}{\sqrt{3}(1-p)} ,$$

$$S_0(E)=\frac{16\pi^2}{\sqrt{3}\,a^2}\left[1-\left[\frac{E-\varepsilon_A}{6V\sqrt{p}}\right]^2\right]$$

$$\text{for } |E-\varepsilon_A|\le 6V\sqrt{p} . \tag{18}$$

Explicit results can also be obtained as $\varepsilon_A\to\infty$ for $E=\varepsilon_A$. In this case the critical concentration p_c is given by

$$p_c=1-2A\int_0^3 dE\frac{\rho_0(E)}{A^2+E^2} , \tag{19}$$

where

$$A=\frac{S_0(0)v_0^2(0)}{35.84} . \tag{20}$$

In Eqs. (19) and (20) we have taken $a=\hbar=2V=1$. For the simple cubic lattice $A=4.64$ and $p_c=0.20$. For the case of Eqs. (12)–(14) we obtain $p_c\simeq 0.193$. It is worthwhile to note that Kolley and Kolley[19] have obtained for the latter case $p_c\simeq 0.50$ using a method simi-

lar to the PWA and employing the simple CPA. The difference is due to their use of a localization criterion which in our notation can be written as

$$Sl_1 l = 12\pi\lambda_E \ . \tag{21}$$

In our PWA method λ_E is always unity, the right-hand side (rhs) constant is equal to 8.96 instead of $12\pi = 37.7$, and l_1 is equal to l. (The difference between l_1 and l is explained in Ref. 13.) It should be noted that our localization criterion [i.e., Eq. (3)] has been repeatedly checked numerically,[13,14] always with very good results, while Eq. (21) has not been checked numerically. Thus the fact that the PWA based on the simple CPA gives too low a value for p_c (even lower than the classical percolation limit) leads us to conclude that it is the *simple* CPA which is responsible for this discrepancy. Indeed the simple CPA, by omitting multiple scattering effects, underestimates the role of disorder. This underestimation is very severe in the present case of binary distribution as it is evident by comparing the simple CPA density of states (see Fig. 5) with the numerical DOS (Fig. 3). As a result the simple CPA mean free path is expected to be much longer than the actual one. Thus we have employed a cluster CPA approach in order to take into account some of the multiple scattering effects omitted in the simple CPA. Our cluster method obtains, in a relatively simple way, g and g_1 and the diagonal and the nearest-neighbor off-diagonal matrix elements of the Green's functions, by considering a cluster of a central site and its nearest neighbors connected to the rest of the lattice which is described by the simple CPA Green's function G as obtained from Eq. (16). The diagonal matrix element g in our cluster method is given by

$$g = \sum_{n=1}^{6} \frac{6!}{(n-1)!(7-n)!} p^{6-n}(1-p)^{n-1} \times \frac{1}{E-\varepsilon_A - 3(7-n)G/8} \ . \tag{22}$$

The off-diagonal matrix element g_1 is obtained from the basic equation $(\hat{E}-\hat{H})g = 1$:

$$g_1 = \frac{1}{6V}[1-(E-\varepsilon_A)g] \ . \tag{23}$$

It is worthwhile to point out that the present cluster CPA although not as sophisticated as others, incorporates certain multiple scattering effects which are very important for states around the middle of the band.

Having g and g_1 we have estimated the cluster CPA mean free path l from the equation

$$\frac{\bar{l}}{l_{\mathrm{CPA}}} = \frac{\ln|G/G_1|}{\ln|g/g_1|} \ , \tag{24}$$

where G and G_1 are the simple CPA results for the diagonal and the nearest-neighbor off-diagonal matrix elements of the Green's function. Equation (24) is based upon the relation $g(n,m) \simeq g \exp(-|n-m|/2\bar{l})$, which is correct for $|n-m| \gg \bar{l}$; n,m are lattice sites. If multiple scattering effects were negligible $g \simeq G$ and $g_1 \simeq G_1$ and consequently $\bar{l} \simeq l_{\mathrm{CPA}}$.

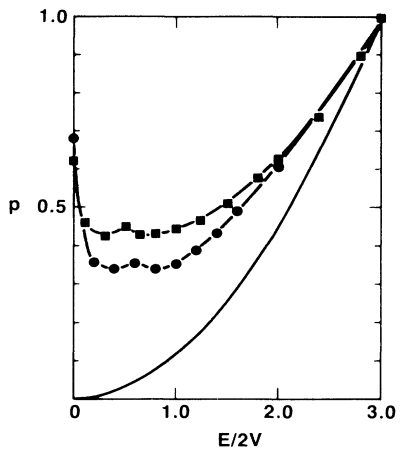

FIG. 4. Mobility-edge trajectory in the concentration energy plane for the binary-alloy model in a simple cubic system. Solid squares are numerical results. Solid circles are the predictions of the PWA based on a cluster CPA. The solid line is the CPA band-edge trajectory.

We have calculated the mobility edge trajectory for the binary disorder case in the limit $\varepsilon_A \to \infty$ using Eq. (3) with $l = \bar{l}$ as in Eq. (24). The results are shown in Fig. 4, where the concentration p_c versus E is plotted. The energy is again measured from the center of the A subband. The solid squares are the numerical results shown in Fig. 2 while the solid circles are the results from the PWA based on the cluster CPA. The agreement between the cluster CPA results and the numerical results for the binary probability distribution of the tight-binding Hamiltonian is rather good. We find only a 10–20% discrepancy and the main features are faithfully reproduced; we remind the reader that for the rectangular and the Gaussian probability distribution the agreement was even better with a discrepancy of less than 5%. In Figs. 5(a), 5(b), and 5(c) we plot the cluster CPA DOS $\rho(E)$, the cluster CPA localization length λ or the correlation length ξ, and the cluster CPA mean free path l as a function of E for three concentrations of $p = 0.20$, 0.35, and 0.40. The shaded regions in $\rho(E)$ in Fig. 5 represent localized eigenstates, while the unshaded regions correspond to extended eigenstates. Notice that around the center of the band the DOS has a small dip, and by construction a δ function exactly at $E = 0$, which is not drawn. The values of l for the cases examined is less than interatomic distances. However, there is a rich structure for λ and ξ at $p = 0.35$, since at this concentration as one increases E from $E = 0$ starts from localized states crosses to extended, then there is a small region of localized states followed by a small region of extended and finally we go into localized and or into the gap. This rich structure reflects the nonmontopic behavior of p_c versus E shown in Fig. 4 with the sharp peak at $E = 0$ and weak maximum at $E/2V \simeq 0.5$. Note that this structure exists both in the numerical data as well the cluster CPA data. However, in the latter appears for lower values of p_c. The structure seen for $E/2V \simeq 0.5$

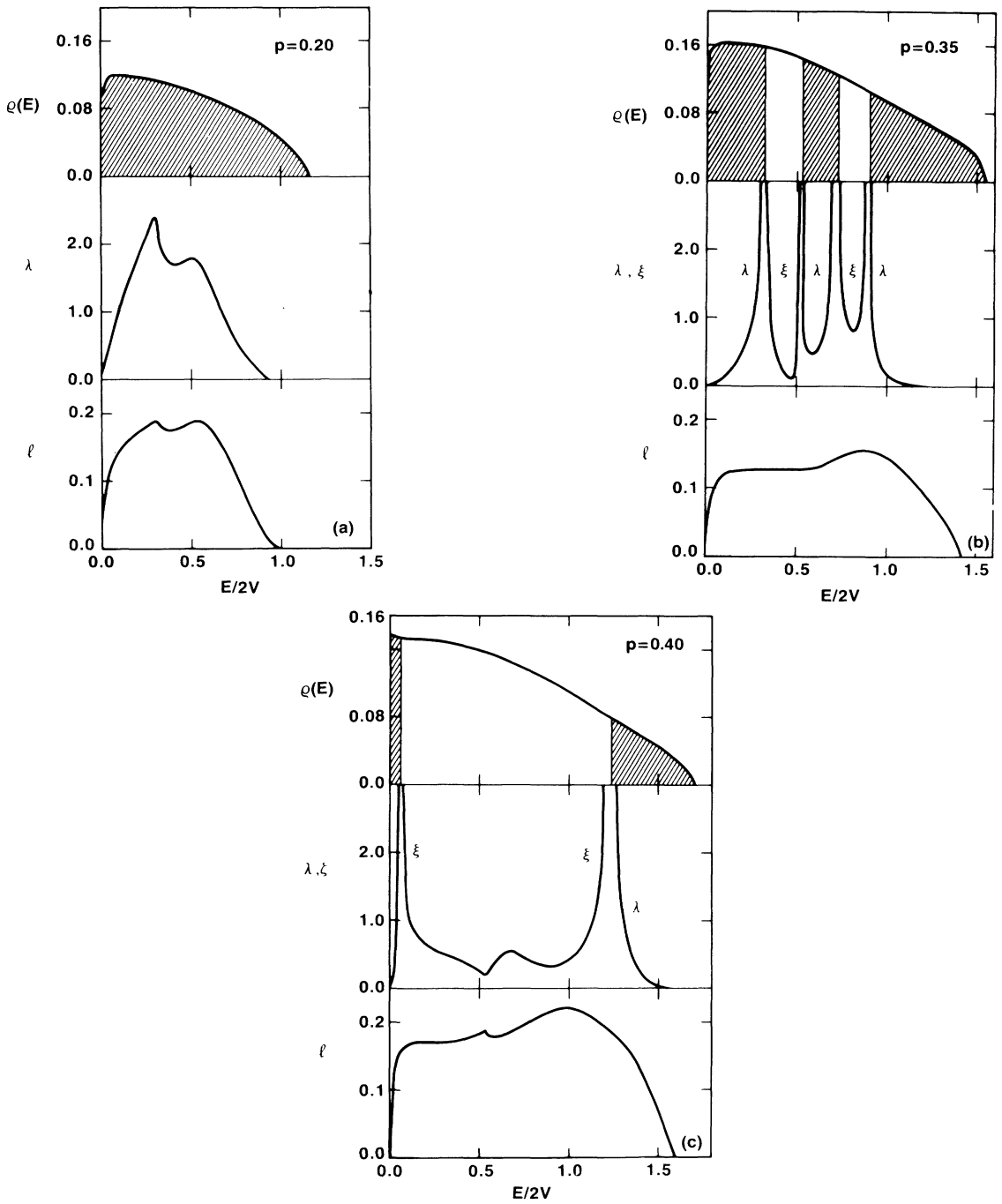

FIG. 5. Results for the density of states $\rho(E)$ localization length λ or correlation length ξ and mean free path l as function of energy for a simple cubic lattice of a binary alloy, within the PWA based on a cluser CPA for (a) $p=0.20$, (b) $p=0.35$, and (c) $p=0.40$.

reflects probably the Van Hove singularity of the unperturbed DOS.

V. CONCLUSIONS

We have calculated the quantum site percolation threshold on a simple cubic lattice not only at the center of the minority subband as in previous studies but in the entire energy region. The mobility trajectory edge in the concentration energy plane for the tight-binding model with a binary-alloy distribution, first calculated by us in this study, is compared with results obtained within the PWA based on a cluster CPA. The agreement between them is satisfactory. Using a new numerical technique, we have calculated the IDOS clearly showing the spike at the center of the subband as well as the gap around it.

The most strikingly result of the present study is summarized in Fig. 2 or Fig. 4, where a nonmonotonic dependence of p_c on E is observed. The most difficult states to localized are not the ones at the center of the subbands (these states are probably localized at any concentration $p \neq 1$ in the limit $\varepsilon_A \to \infty$) but the states at $E/2V \simeq 0.3$.

ACKNOWLEDGMENTS

This work was partially supported by North Atlantic Treaty Organization Grant No. RG684/84. Ames Laboratory is operated for the United States Department of Energy by Iowa State University under Contract No. W-7405-Eng.82.

*Permanent address: Ames Laboratory and Department of Physics, Iowa State University, Ames, IA 50011.

†Permanent address: Research Center of Crete and Department of Physics, University of Crete, Heraklio, Crete, Greece.

[1]S. Kirkpatrick and T. P. Eggarter, Phys. Rev. B **6**, 3598 (1972).

[2]T. Odagaki, N. Ogita, and H. Matsuda, J. Phys. C **13**, 189 (1980).

[3]R. Ragharan and D. C. Mattis, Phys. Rev. B **23**, 4791 (1981).

[4]Y. Shapir, A. Aharony, and A. B. Harris, Phys. Rev. Lett. **49**, 486 (1982).

[5]R. Raghavan, Phys. Rev. B **29**, 748 (1984).

[6]V. Srivastava and M. Chaturvedi, Phys. Rev. B **30**, 2238 (1984).

[7]T. Odagaki and K. C. Chang, Phys. Rev. B **30**, 1612 (1984).

[8]L. Root and J. L. Skinner, Phys. Rev. B **33**, 7738 (1986).

[9]D. W. Heermann and D. Stauffer, Z. Phys. B **44**, 339 (1981).

[10]J. L. Pichard and G. Sarma, J. Phys. C **14**, L127 (1981); A. Mackinnon and B. Kramer, Phys. Rev. Lett. **47**, 1546 (1981); Z. Phys. B **53**, 1 (1983).

[11]C. M. Soukoulis, I. Webman, G. S. Grest, and E. N. Economou, Phys. Rev. B **26**, 1838 (1982).

[12]A. D. Zdetsis, C. M. Soukoulis, E. N. Economou, and G. S. Grest, Phys. Rev. B **32**, 8711 (1985); C. M. Soukoulis, A. D. Zdetsis, and E. N. Economou, Phys. Rev. B **34**, 2253 (1986).

[13]E. N. Economou and C. M. Soukoulis, Phys. Rev. B **28**, 1093 (1983); **30**, 1686 (1984).

[14]E. N. Economou, C. M. Soukoulis, M. H. Cohen, and A. D. Zdetsis, Phys. Rev. B **31**, 6483 (1985).

[15]E. N. Economou, *Green's Functions Quantum Physics*, 2nd ed. (Springer, Heidelberg, 1983).

[16]R. J. Elliot, J. A. Krumhansl, and P. L. Leath, Rev. Mod. Phys. **46**, 437 (1974); and references therein.

[17]D. C. Licciardello and E. N. Economou, Phys. Rev. B **11**, 3697 (1975).

[18]Q. Li and C. M. Soukoulis (unpublished).

[19]E. Kolley and W. Kolley, Phys. Status Solidi B **135**, K89 (1986).